Published in final edited form as:
*Cell Calcium*. 2014 February ; 55(2): 93–103. doi:10.1016/j.ceca.2013.12.004.

# Activity of nicotinic acid substituted nicotinic acid adenine dinucleotide phosphate (NAADP) analogs in a human cell line: difference in specificity between human and sea urchin NAADP receptors

**Ramadan A. Ali**[‡,1], **Tetyana Zhelay**[†], **Christopher J. Trabbic**[‡,1], **Timothy F. Walseth**[§], **James T. Slama**[‡], **David R. Giovannucci**[†,*], and **Katherine A. Wall**[‡,*]

[‡]Department of Medicinal and Biological Chemistry, College of Pharmacy and Pharmaceutical Sciences, University of Toledo Health Sciences Campus, 3000 Arlington Avenue, Toledo, Ohio 43614

[†]Department of Neurosciences, University of Toledo Health Sciences Campus, 3000 Arlington Avenue, Toledo, Ohio 43614

[§]Department of Pharmacology, University of Minnesota Medical School, Minneapolis, Minnesota 55455

## Summary

Nicotinic acid adenine dinucleotide phosphate (NAADP) is the most potent $Ca^{2+}$ mobilizing second messenger that has been identified. We have previously shown that NAADP analogs substituted at the 5-position of nicotinic acid were recognized by the sea urchin receptor at low concentration, whereas the 4-substituted analogs were not as potent. However, to date the structure activity relationship (SAR) of these analogs has not been addressed in mammalian systems. Thus, we asked whether these structurally modified analogs behave similarly in an NAADP-responsive mammalian cell line (SKBR3) using microinjection and single cell fluorescent imaging methods. Novel "caged" 4- and 5- substituted NAADP analogs that were activated inside the cell by flash photolysis resulted in $Ca^{2+}$ mobilizing activity in SKBR3 cells in a concentration dependent manner, but with reduced effectiveness compared to unmodified NAADP. The SAR in mammalian SKBR3 cells was quite different from that of sea urchin and may suggest that there are differences between NAADP receptors in different species or tissues. Importantly, these data indicate that modifications at the 4- and 5-position of the nicotinic acid ring may lead to the development of functional photoaffinity labels that could be used for receptor localization and isolation in mammalian systems.



[*]To whom correspondence should be addressed: KAW Phone: 419.383.1943, Fax: 419.383.1909, katherine.wall@utoledo.edu.; DRG Phone 419.383.5004, Fax 419.383.3008, david.giovannucci@utoledo.edu.

[1]Submitted in partial fulfillment of the requirements for the doctoral degree in Medical Chemistry, University of Toledo College of Graduate Studies

**Keywords**

NAADP; Structure-Activity Relationships; Antagonists; Caged-NAADP; SKBR3 cells; $Ca^{2+}$ signaling

## 1. Introduction

$Ca^{2+}$ release from intracellular stores is an important event controlling several cellular processes and regulating many different functions [1–3]. In addition to the well-known intracellular $Ca^{2+}$ release mechanisms triggered by inositol-1,4,5 triphosphate ($IP_3$) and cyclic ADP-ribose (cADPR), that target inositol triphosphate and ryanodine receptors (RyR) on the endoplasmic reticulum, respectively [4–7], nicotinic acid adenine dinucleotide phosphate (NAADP) has emerged as the most potent $Ca^{2+}$ mobilizing messenger [8]. NAADP was originally discovered as a contaminant of commercial NADP [9] and introduced as a $Ca^{2+}$ releasing messenger in sea urchin eggs active at nanomolar concentrations [10]. Later, NAADP-dependent $Ca^{2+}$ mobilizing activity was observed in different cell types and mammals including pancreatic acinar cells [11], heart [12], brain [13], kidney [14], lymphocytes [15], and human transformed Jurkat T cells [16]. In contrast to $Ca^{2+}$ release in response to $IP_3$, the nature of the NAADP targeted intracellular $Ca^{2+}$ store as well as the identity of its receptor is not established [17]. For example, NAADP-induced $Ca^{2+}$ release has been shown to differ in many ways from either $IP_3$ or cADPR-mediated $Ca^{2+}$ release [10, 16, 18–20]. Most available evidence suggests that NAADP-induced $Ca^{2+}$ release occurs from a different subcellular compartment than does $Ca^{2+}$ release in response to $IP_3$ or cADPR [21]. Unlike canonical $Ca^{2+}$ releasing messengers, NAADP mobilizes $Ca^{2+}$ from acidic stores [22–24] although it appears to crosstalk with canonical intracellular channels or directly release $Ca^{2+}$ from the ER in some cells [25, 26].

Because NAADP signaling is found in a diverse array of species and tissues, it is possible that the receptor differs according to its source. In addition, the structural features of NAADP required for agonist recognition are only now being defined [27]. A recent study showed that substitution at the 4-position of the nicotinic acid resulted in the loss of agonist potency for both $Ca^{2+}$ release and ligand binding in sea urchin egg homogenates, whereas substitution at the 5-position was tolerated [28]. The structural features of NAADP which are necessary for receptor recognition have been best characterized in sea urchin egg homogenates, and include the adenosyl-2′-phosphate, the purine-6-nitrogen, and the pyridine-3-carboxylate [29, 30]. In mammalian cells, the structure activity relationship (SAR) for NAADP recognition is virtually unknown due to the impermeability of NAADP and to the absence of robust cell-free preparations [31]. Only one NAADP analog has so far been tested, the 5-$N_3$-NAADP reported to be active in cultured human cells by microinjection [32]. In this report, we have synthesized inactive “caged” NAADP analogs [33, 34] that are activated inside the cell by flash photolysis and characterized their ability to mobilize $Ca^{2+}$ via the NAADP receptor in the mammalian cell line SKBR3 using microinjection and single cell fluorescent imaging methods.

## 2. Results

### 2.1 Synthesis and characterization of caged NAADP derivatives

NAADP is highly negatively charged and cannot cross the plasma membrane of intact cells in the absence of pores or a specific transport system. Also, direct microinjection of NAADP requires specialized apparatus, and may cause an injection artifact which can skew experiment results if the response is monitored simultaneously with injection. Moreover, receptor desensitization by sub-threshold concentrations might occur as a result of unequal distribution of NAADP throughout the cell. This poses immense difficulties in experiments to investigate its role in its natural environment and to understand the underlying mechanism of NAADP/$Ca^{2+}$ release. For these reasons, the use of inactive photolabile caged NAADP that can be activated when necessary by photolysis is the ideal molecular tool for more controlled delivery and investigation of NAADP. To achieve this goal, we have begun using caged NAADP (**1**), in which a 1-(4,5-dimethoxy-2-nitrophenyl)ethyl caging group is attached as an ester to the adenosyl-2′-phosphate. The synthesis of (DMNPE)-NAADP was based on a previously published study [33] (Fig. 1) and involved reaction of the 2′-phosphate of NADP with 4,5-dimethoxy-2-nitrophenyl diazoethane (DMNPE) yielding caged NADP. This was converted to the caged NAADP (**1**) by enzyme catalyzed exchange of nicotinic acid for nicotinamide using the activity of *Aplysia californica* ADP-ribosyl cyclase [35] to produce the corresponding caged NAADP derivatives. Since substituted nicotinic acids are readily available [28], caged NAADP derivatives **2–5** were synthesized in one step through the common intermediate DMNPE-caged NADP using enzyme catalyzed base exchange.

Although all analogs under study were esterified with the same caging group and therefore were expected to have similar photolysis rates, we investigated the possibility that the photolysis rates of these analogs might be different. Solutions of pure caged analogs of equal concentration were photolysed under controlled identical conditions using a short wave ultraviolet lamp and the resulting product mixture was analyzed by HPLC (Fig. 2A). The ratio of the amount of photolysed product to the intact analog was determined, and as expected, the uncaging efficiencies between analogs were not significantly different (Fig. 2B). The separated compounds can be differentiated by both their mobilities on anion exchange chromatography and their ultraviolet spectra (Supplementary Material Fig. S1).

To demonstrate that the caged NAADP and derivatives were unable to stimulate $Ca^{2+}$ release and remained intact inside the cell, we examined $Ca^{2+}$ release in sea urchin egg homogenates as previously described [36]. The addition of 93 nM caged NAADP caused no $Ca^{2+}$ release by the homogenates (Fig. 2C). The addition of the same amount of caged NAADP that had been UV irradiated in a Rayonet photochemical reactor for 2 minutes caused significant $Ca^{2+}$ release. Similarly, caged 5-methyl-NAADP caused $Ca^{2+}$ release only after UV irradiation (Fig. 2D).

### 2.2 NAADP induces $Ca^{2+}$ release from SKBR3

Our goal was to study the effect of chemical modification at the 4- and 5-nicotinic acid of NAADP in mammalian systems and compare it to the biological activity previously

observed in sea urchin eggs. To achieve this, we used the human breast cancer cell line SKBR3, which has been previously shown to respond to NAADP [37, 38]. This system allowed us to study the effect of flash photolysis of caged NAADP on the intracellular $Ca^{2+}$ concentration $[Ca^{2+}]_i$. To determine the concentration response–relationship, we injected a known concentration of caged NAADP into single cells and monitored $[Ca^{2+}]_i$ fluorometrically using the calcium sensitive dye Fluo-4. Microinjection of caged NAADP at a pipette concentration as low as 10 nM followed by 8 to 10 flashes of ultraviolet light causing photorelease of NAADP elicited a $Ca^{2+}$ response, whereas ultraviolet flashes of intracellular buffer alone had no effect (Fig. 3A). The stepwise nature of the fluorescence reflects accumulating uncaged NAADP with each flash of UV light. Within each experiment, the same number of flashes was used. As shown in Fig. 3B, the concentration response relationship showed a bell-shaped curve for the $Ca^{2+}$ peak with an optimal caged NAADP pipette concentration at 100 nM. These data are consistent with other cellular systems and with the observation that NAADP induces $Ca^{2+}$ release at low 30 – 100 nM concentrations, but desensitizes at high micromolar concentrations [10, 11, 16, 18, 39].

### 2.3 Extracellular calcium is not involved in NAADP signaling

After establishing that photolysis of caged NAADP evoked $Ca^{2+}$ signals in a concentration dependent manner, we investigated the dependence of the evoked signals on extracellular $Ca^{2+}$. To determine whether $Ca^{2+}$ entry is involved in the NAADP-mediated $Ca^{2+}$ response, we monitored cytosolic $Ca^{2+}$ evoked by 100 nM caged NAADP in $Ca^{2+}$-free medium. As shown in Fig 4 A and B, the $Ca^{2+}$ signal was similar to that observed in $Ca^{2+}$-containing medium and consistent with the result observed in pancreatic acinar cells [11]. This finding indicates that most of the $Ca^{2+}$ was released from internal stores. It is worth noting that the response was reduced when the cells were suspended in $Ca^{2+}$-free medium for a prolonged time period, greater than 15 minutes. This was likely due to a reduction in intracellular $Ca^{2+}$ content of the cell during prolonged suspension in $Ca^{2+}$ free medium, as has been previously reported [40].

### 2.4 ER contribution to NAADP-$Ca^{2+}$ signaling in SKBR3

We next focused on the intracellular $Ca^{2+}$ stores involved, since extracellular $Ca^{2+}$ did not to play any major role in NAADP evoked signals. The major intracellular $Ca^{2+}$ stores proposed to participate in NAADP-mediated $Ca^{2+}$ signaling are the ER and acidic stores. We first examined the role of the ER $Ca^{2+}$ store and sought to determine whether it was directly released in response to NAADP or indirectly involved through $Ca^{2+}$ induced $Ca^{2+}$ release. To test whether $Ca^{2+}$ stored in the endoplasmic reticulum contributed to NAADP-$Ca^{2+}$ signaling, we monitored the effect of photorelease of NAADP on the cytosolic $Ca^{2+}$ concentration after the depletion of $Ca^{2+}$ from the ER store using known inhibitors of the SERCA-ATPase pump, thapsigargin (TG) and cyclopiazonic acid (CPA). Depleting the ER store by pretreatment with CPA reduced the fluorescence associated with the NAADP response by 40 percent compared to control (Fig. 4 C and D). Similarly, depleting the ER by pretreatment with thapsigargin reduced the NAADP-induced $Ca^{2+}$ response by 40 percent compared to control (Data not shown).

Previous experiments with Jurkat cells [26, 41] demonstrated a role for the ryanodine receptor in NAADP-dependent $Ca^{2+}$ release. We examined the involvement of the ryanodine receptor in SKBR3 cells by pretreating the cells with tetracaine, a ryanodine receptor antagonist, prior to stimulation. Tetracaine reduced the subsequent response to NAADP by about 30% (Fig. 4 E), similar to the effect of CPA. This indicates that the ryanodine receptor is likely involved in the NAADP effect on ER release.

To support our observation that the ER is in fact contributing to the NAADP-induced $Ca^{2+}$ signal, we indirectly examined the level of $Ca^{2+}$ content in the ER before or after a response to NAADP uncaging. For example, we compared the rise in intracellular $Ca^{2+}$ concentrations induced by CPA applied before or after the photorelease of NAADP. When NAADP was photoreleased prior to CPA application, the response to CPA was reduced by about 50% compared to the response when CPA was applied prior to photorelease (data not shown). Consistent with this observation, extracellular application of 100 μM ATP to activate ER $Ca^{2+}$ release before the photorelease of NAADP induced robust $Ca^{2+}$ signals in control cells, but the ATP-evoked signal was diminished when applied following the photolytic release of NAADP (Fig. 4F). This suggests that some ATP sensitive stores are reduced by NAADP induced $Ca^{2+}$ release. Together these data indicate that a portion of $Ca^{2+}$ released in response to NAADP uncaging was from the ER.

### 2.5 Acidic stores are the dominant source of NAADP evoked $Ca^{2+}$ release in SKBR3

Since the depletion of $Ca^{2+}$ from ER stores did not eliminate the signal, we investigated the role of endosomes and lysosomes in the NAADP-mediated $Ca^{2+}$ release. We depleted the endo-lysosomal $Ca^{2+}$ using the vacuolar proton pump ($H^+$-ATPase) inhibitor bafilomycin A1 (confirmed by loss of Lysotracker Red accumulation, not shown) and monitored $[Ca^{2+}]_i$ after the injection of an optimal caged NAADP concentration (100 nM) and photolysis. The $Ca^{2+}$ signal observed following bafilomycin treatment was greatly reduced (five-fold lower than the control response) as shown in Fig. 5 A and B. These results are consistent with previous data from SKBR3 [37, 38] and indicate that the $Ca^{2+}$ store mobilized by NAADP was reduced by the depletion of $Ca^{2+}$ from the endo-lysosomal lumen. Thus, lysosome-like acidic stores appeared to be the dominant source of NAADP evoked $Ca^{2+}$ release in SKBR3.

### 2.6 BZ194 antagonizes NAADP-mediated $Ca^{2+}$ in SKBR3

We also investigated the effect of the NAADP antagonist BZ194 on the response induced by the photorelease of NAADP to confirm that the $Ca^{2+}$ signals are indeed mediated by NAADP. BZ194 was reported to antagonize NAADP-mediated $Ca^{2+}$ signaling via the type 1 ryanodine receptor in Jurkat T lymphocytes [26]. The response of SKBR3 cells to NAADP was diminished when 100 μM of BZ194 was co-injected along with the optimal concentration of caged NAADP (Fig. 6A). The inhibition by BZ194 of the NAADP response was concentration dependent (Fig. 6B) which provides evidence that the $Ca^{2+}$ signals are due to the photorelease of NAADP. Interestingly, BZ194 did not inhibit NAADP-mediated $Ca^{2+}$ release (Fig. 7 A and B) nor demonstrate any binding affinity for the NAADP receptor in sea urchin egg homogenates (Fig. 7C). The NAADP analog Ned-19 [42] was also found to be inactive in this preparation. Three separate lots of Ned-19 were

tested on *S. purpuratus* egg homogenates, and concentrations of Ned-19 up to 1.6 μM, when pre-incubated with the homogenate for 2–3 min, failed to inhibit $Ca^{2+}$ release in response to added NAADP (data not shown). Ned-19 at concentrations up to 10 μM similarly failed to inhibit the binding of [$^{32}$P]NAADP to *S. purpuratus* membranes in the competition ligand binding assay (data not shown).

### 2.7 Structure activity relationship in a mammalian system

In sea urchin eggs, substitution of NAADP at the 4-position of the nicotinic acid resulted in the loss of agonist potency for both $Ca^{2+}$ release and ligand binding, whereas substitution at the 5-position was tolerated [28]. To determine the effects of modification of NAADP at the 4- and 5-position of nicotinic acid in a mammalian system, we constructed concentration response curves for NAADP analogs **(2–5)** modified at the 4- and 5-position of the nicotinic acid moiety.

In SKBR3 cells the photolysis of caged 4-methyl-NAADP **(2)** elicited an optimal response at a pipette concentration of 100 nM (Fig. 8). The evoked $Ca^{2+}$ response after photolysis of caged 4-methyl-NAADP **(2)** showed concentration dependence similar to that of caged NAADP (Fig. 8). Although uncaged 4-methyl-NAADP **(2)** is approximately equipotent with uncaged NAADP **(1)**, the magnitude of $Ca^{2+}$ release at optimal concentration of **(2)** is approximately 50% lower than that elicited by uncaged NAADP **(1)**.

Interestingly, the maximal response observed after the photolysis of caged 5-methyl-NAADP **(3)** was at a pipette concentration of 10 μM, indicating that it is 100-fold less potent than the parent compound NAADP **(1)**. As shown in Fig. 8, the evoked changes in cytosolic $Ca^{2+}$ concentration increased in a concentration dependent manner that exhibited a maximal response at 10 μM. Above this concentration, the evoked signal gradually diminished. In addition, we tested two more analogs modified at the 5-position of nicotinic acid to determine whether this modification reduced the potency of the analogs in the mammalian system. Both analogs, 5-amino-NAADP **(4)** and 5-thiomethyl-NAADP **(5)**, elicited the maximal response at a pipette concentration of 100 nM but with a reduced efficacy (Fig. 8). The concentration responses of 5-amino-NAADP **(4)** and 5-thiomethyl-NAADP **(5)** had similar shapes to that of NAADP with 2-fold and 5-fold less efficacy, respectively. These data demonstrated that substitution at the 5-position of nicotinic acid of NAADP exhibits a similar bell shaped concentration response relationship but with significantly reduced efficacy of $Ca^{2+}$ release.

## 3. Discussion

We report a chemo-enzymatic synthesis of four novel photolabile caged NAADP derivatives. Each of these compounds was synthesized in a single step from the common intermediate DMNPE-caged NAADP and a 4 or 5-substituted nicotinic acid derivative using the enzyme catalyzed pyridine base exchange reaction. The novel caged NAADP derivatives **(2–5)** were purified by anion exchange chromatography, shown to be homogeneous by HPLC, and were characterized using NMR and mass spectrometry (shown in Supplementary Material Figures S7-S10). Caged NAADP derivatives **(2–5)** were found to be stable during storage as solid dry powders at −80 °C, and were deprotected after 10 minutes of irradiation

with UV light at identical amounts. Although these polar anionic compounds are not expected to traverse cell membranes, they can be delivered intracellularly in a controlled manner by microinjection, thus enabling the role of NAADP in its cellular environment and the underlying mechanism of NAADP/$Ca^{2+}$ release to be investigated.

In our initial experiments, we observed intracellular $Ca^{2+}$ release from SKBR3 cells in response to the photolysis of microinjected caged NAADP **(1)**. In accord with previous observations [10, 11, 16, 18, 39], the concentration–response relationship was bell shaped, indicative of inhibition at high NAADP concentration. The concentration of microinjected **(1)** that evoked a maximum $Ca^{2+}$ response was found to be 100 nM. This concentration was comparable to that previously reported to activate $Ca^{2+}$ release in mammalian cells.

We next demonstrated that $Ca^{2+}$ release in SKBR3 cells in response to photolysis of caged NAADP **(1)** showed similar pharmacological characteristics to the response to microinjected uncaged NAADP. The $H^+$-ATPase pump inhibitor bafilomycin A abolished the response to photolysed NAADP, indicating that lysosome-like acidic stores are the dominant source of NAADP evoked $Ca^{2+}$ release in SKBR3 cells. This agrees with the bulk of current evidence that NAADP targets acidic stores to trigger $Ca^{2+}$ release [43]. However, since depletion of ER stores by thapsigargin or cyclopiazonic acid prior to NAADP uncaging reduced the response, ER stores must also be involved. The contribution of ER stores to the overall NAADP response was confirmed with reversal of the order of addition. NAADP uncaging prior to CPA or ATP addition reduced subsequent responses to CPA or ATP, showing reduction of ER stores. Involvement of the ryanodine receptor is suggested by the reduction of the NAADP response by tetracaine treatment. These data support the hypothesis that the ER is indirectly involved via $Ca^{2+}$ induced $Ca^{2+}$ release and that the initial $Ca^{2+}$ signal raised or “triggered” by NAADP is dependent on acidic stores and is necessary for the ER contribution for the propagation of that signal. Cross-talk between calcium stores exists in many cell types [24, 43, 44] and it has been speculated that NAADP has a role in initiating rather than propagating calcium signals and that the initial signal is derived from NAADP-mediated release from acidic stores and amplified by ryanodine receptors through the process of $Ca^{2+}$-induced $Ca^{2+}$ release [11]. Our findings are consistent with this proposal.

Based on the average 15 μm size of SKBR3 cells[45], we estimate that we are microinjecting 1 to 10% of the cell volume. Due to the inability to measure the light at the plane of focus, we cannot directly determine the concentration of photolysed NAADP present in the cell. However, each flash must release only a small portion of the total, since subsequent flashes release more $Ca^{2+}$ and a second train of flashes given following rest will again release more $Ca^{2+}$. The local nature of the release is shown by the relaxation of the response in contrast to the sustained $Ca^{2+}$ concentrations seen in some cells with microinjected NAADP. However, the amount of each analog relative to other analogs should be constant.

We report the effect of introducing substituents into the pyridine base ring of NAADP at the 4- or the 5-positions on the ability of the analog to induce $Ca^{2+}$ release in a mammalian cell line (SKBR3) and compare it to a previous SAR study in sea urchin eggs to help understand NAADP receptor diversity across species (see Table 1). In sea urchin eggs, the 5-substituted

nicotinic acid NAADP analogs were found to be well recognized by the receptor and elicited $Ca^{2+}$ release at low concentrations, whereas the 4-substitued analogs were found to lose agonist potency [28]. In SKBR3 cells, we found that 4- and 5-substituted analogs both have $Ca^{2+}$ ion mobilizing activity. 4-Methyl-NAADP (from uncaging of **2**), which was found to be 2000-fold less potent than NAADP in sea urchin eggs, induced $Ca^{2+}$ release at low nanomolar concentrations approximately equipotent with NAADP, but was twofold less effective than NAADP itself in eliciting maximal $Ca^{2+}$ release from SKBR3 cells. Comparison of this particular analog in sea urchin eggs and in mammalian SKBR3 cells suggests a major difference between the two systems in terms of tolerance to substitution at the nicotinic acid 4-position. This difference was notable, since all the 4-substituted analogs tested in sea urchin eggs lost potency for $Ca^{2+}$ release and receptor binding activity. The different behavior of 4-methyl-NAADP in sea urchin eggs and the mammalian cell line SKBR3 suggests differences in the binding site between species. However, it is important to note that the $Ca^{2+}$ release studies are done in cellular homogenates of sea urchin eggs and with intact cells for the mammalian receptor. Recently, photoaffinity labeling of NAADP targets in homogenates of sea urchin eggs and of the mammalian cell lines SKBR3 and Jurkat showed different molecular masses of the photolabeled proteins [32, 46, 47]. This suggests that differences are inherent in the receptors themselves. The activity of other analogs with different substitutions at the 4-position will be investigated in future experiments in an attempt to produce more potent NAADP analogs for the mammalian system. The 5-substituted NAADP analogs were slightly less effective than NAADP and none were able to elicit more than 50% of the $Ca^{2+}$ release produced by NAADP itself in SKBR3 cells. Their relative potencies are comparable in both systems, with the exception of 5-methyl-NAADP. 5-Methyl-NAADP was approximately equipotent with NAADP in sea urchin eggs [28] and its activity in SKBR3 seemed to be the opposite of its activity observed in sea urchin eggs. 5-Methyl-NAADP was 100-fold less potent than NAADP in SKBR3 compared to 2.3-fold less potent in sea urchin eggs. Likewise in SKBR3, while 5-methyl-NAADP was 100-fold less potent than NAADP, 5-amino-NAADP and 5-thiomethyl-NAADP were both tolerated with only two and five fold loss of efficacy respectively.

BZ194 was reported to antagonize NAADP-mediated $Ca^{2+}$ signaling via the type 1 ryanodine receptor in Jurkat T-lymphocytes [26]. The role of BZ194 in antagonizing NAADP-mediated $Ca^{2+}$ release in SKBR3 cells seems to be through a different mechanism. Since lysosome-like acidic stores appeared to be the dominant source of NAADP evoked $Ca^{2+}$ release in SKBR3 as demonstrated above, it suggests that NAADP does not to bind RyR directly but activates novel channels located on acidic stores and thus the antagonism effect by BZ194 is not likely to be directly via RyR. Another possibility is that BZ194 indeed modulates its antagonistic effect on NAADP-mediated $Ca^{2+}$ release via RyR by inhibiting the propagation of $Ca^{2+}$ signals. This is not likely because BZ194 exhibited a much larger inhibition compared to that caused by $Ca^{2+}$ depletion from the ER or by tetracaine, and similar to that of bafilomycin A.

We find that the four simple substituted NAADP derivatives tested differ in activity between sea urchin and SKBR3 cells both with respect to relative potencies and with respect to efficacy. We also observe a difference between sea urchin and SKBR3 cells with respect to

sensitivity to the antagonist BZ194. BZ194 did not show any antagonist activity for NAADP-mediated $Ca^{2+}$ signaling nor show any binding affinity for the NAADP receptor in sea urchin egg homogenates. Our observations imply a different SAR with respect to recognition at the 4-position of the nicotinic acid moiety between sea urchin eggs and mammalian cells at least in SKBR3. They indicate that the NAADP receptor exhibits diversity across species and among tissues. They also suggest that further modifications at the 4- and 5-position of the nicotinic acid ring may lead to the development of reagents for future studies of the NAADP-induced $Ca^{2+}$ release system, including potent agonists and photoaffinity labels that could be used for receptor localization and isolation in mammalian systems.

## 4. Materials and methods

### 4.1 General description

The following procedures were used in all reactions unless otherwise noted. Reactions were performed in clean oven-dried glassware. All light sensitive reactions were carried out in the dark and the products were protected with aluminum foil and stored at −80 °C. Reactions were stirred using Teflon-coated magnetic stir bars. Chemical reagents were purchased from either Sigma-Aldrich or Acros Organics and used as received. $MnO_2$ was from EM Sciences-Darmstadt, Germany. All reagent grade solvents (acetone, ethanol, methanol, ethyl acetate, and hexane) were purchased from Pharmco-AAPER or EMD chemicals. All anhydrous solvents were purchased in sure seal bottles from Sigma-Aldrich. Bafilomycin A1 was purchased from LC Laboratories, thapsigargin from Calbiochem, CPA from Sigma-Aldrich, Lysotracker Red from Molecular Probes, and Fluo-4 from Invitrogen. Proton $^{1}H$ NMR spectra were measured in $CDCl_3$ or $D_2O$ and determined using either a Unity-400 spectrophotometer (400 mHz) or a Varian Inova-600 spectrophotometer (600 mHz). All chemical shifts are reported in the standard (δ) notation of parts per million (ppm) and were referenced to the residual proton signal of the deuterated solvent, and reported to the second decimal place. $^{31}P$ NMR was recorded on a Unity-400 spectrophotometer (162 mHz) with 85 % $H_3PO_4$ as an external reference. High-resolution mass spectral analyses were carried out at the Ohio State Mass Spectrometry & Proteomics Facility using either ESI or MALDI-TOF mass spectrometry.

### 4.2 HPLC analysis

The system for analysis of nucleotides using AG MP-1 anion exchange chromatography in gradient of trifluoroacetic acid and water was originally described in Axelson et.al. [48].

**Method 1: Analytical column—**To monitor the progress of caging and base-exchange reactions and to determine the purity of caged NAADP and its derivatives after purification, a Bio-Rad Uno-Q column (7 × 35 mm, 1.3 ml of anion-exchange resin) fitted to a Bio-Rad BioLogic Duoflow HPLC apparatus was used. Samples were injected into a loop with a volume of 50 µl. The flow rate throughout was 3 ml/min. Sample concentration was roughly equal to1mg/ml. Solvent A: $H_2O$; Solvent B: 100 mM aqueous TFA: detection at 254 nm. 1) Load/inject sample, 50µl; 2) Solvent A, 9 ml; 3) Linear gradient, 0–50 % solvent B formed

over 30 ml; 4) Solvent B, 9 ml; 5) Solvent A, 9ml. The total volume of this procedure is 57 ml.

**Method 2: Prep-scale column—**For purification purpose following large scale synthesis reactions of caged NAADP and its derivatives, a glass column (1.5 × 11.5 cm) filled with Bio-Rad AG-MP 1ion-exchange resin was connected with a Bio-Rad BioLogic Duoflow HPLC apparatus was used. The sample was introduced using an injection loop with a volume of 5 ml. The flow rate throughout was 5 ml/min. The sample concentration was roughly equal to 5 mg/ml. Solvent A: $H_2O$; Solvent B: 100 mM aqueous TFA: detection at 254 nm. 1) Load/inject sample, 5 ml; 2) Solvent A, 10 ml; 3) Linear gradient, 0–60 % solvent B formed over 120 ml; 4) Solvent B, 10 ml; 5) Solvent A, 10 ml. The total volume of this procedure is 155 ml.

### 4.3 Synthesis of NAADP analogs

**Synthesis of 5-thiomethyl nicotinic acid—**5-Bromonicotinic acid (1 g, 5 mmol), sodium thiomethoxide (385 mg, 5.5 mmol) (Sigma-Aldrich) and dimethylformamide (10 ml) were added to a 10–20 ml Biotage microwave reactor vial. The vial was properly capped and allowed to react for 24 hours at 200 °C. After this time, TLC clearly revealed the presence of starting material. Another portion of sodium thiomethoxide (385 mg, 5.5 mmol) was added and allowed to react for 24 hours at 200 °C. The reaction was now shown to be complete and the crude material was filtered through Celite. The Celite was washed with 100 ml of 50% methanol in dichloromethane (DCM). The filtrates were combined and the solvent was evaporated *in vacuo*. The resulting residue was purified by column chromatography on silica gel (97:2:1 DCM:MeOH: acetic acid) affording a white solid (480 mg, 57 %): TLC R*f* 0.49 in DCM: MeOH: acetic acid (95:4:1), $^1$H NMR (400 mHz, $CD_3OD$) δ 8.85 (s, 1H), 8.60 (s, 1H), 8.22 (s, 1H), 2.59 (s, 3H); $^{13}$C NMR (100 mHz, $CD_3OD$) δ 151.1, 147.4, 135.9, 15.2. HRMS calcd for $C_7H_7NO_2S$: 170.0276 (M+H), Found *m/z*: 170.0278 (M+H). Structure, NMR traces and HRMS shown in Figure S2.

**Synthesis of 4,5–dimethoxy-2-nitroacetophenone—**4,5-Dimethoxyacetophenone (3 g, 16.6 mmol) was added over 10 min to concentrated nitric acid (20 ml) cooled using an ice-bath. The solution was stirred for 1 h and then poured into cold water (200 ml) to precipitate the product. The product was collected by filtration and recrystallized from ethanol (1 g, 27%); $^1$H NMR ($CDCl_3$, 600 MHz): δ 7.63 (s, 1H), 6.77 (s, 1H), 3.99 (s, 6H), 2.51 (s, 3H); mp found 130–133°C; reported mp 130–132 °C [49]. Structure and NMR shown in Figure S3.

**Synthesis of 4,5-dimethoxy-2-nitroacetophenylhydrazone—**4,5-Dimethoxy-2-nitroacetophenone (250 mg, 1 mmol) was dissolved in ethanol (15 ml); acetic acid (180 mg, 3 mmol) was added and the mixture was stirred for 10 min at room temperature. Hydrazine monohydrate (160 mg, 5 mmol) was added and the resulting solution was refluxed for 3 h. After cooling to room temperature, the solvent was evaporated under reduced pressure and the crude product was partitioned between water and chloroform several times. The chloroform was evaporated and the product was recrystallized from toluene and dried under vacuum to give a yellow powder (200 mg, 76%). $^1$H NMR ($CDCl_3$, 600 MHz): δ 7.59 (s,

1H), 6.85 (s, 1H), 5.37 (bs, 2H), 3.95 (s, 6H), 2.01(s, 3H). Structure and NMR shown in Figure S4.

**Synthesis of DMNPE-caged NADP—**A solution of NADP (74.4 mg, 0.1 mmol) in water (3 ml) was adjusted to pH 4 with NaOH (1.0 M) and placed in a 10 ml reaction vial. 4,5-Dimethoxy-2-nitroacetophenylhydrazone (0.2 g, 0.84 mmol) in chloroform (2 ml) was stirred in a separate reaction vial with $MnO_2$ (0.8 g, 8.4 mmol, EM Sciences, Darmstadt, Germany) for 10 min in the dark. The resulting dark red chloroform solution of 4,5-dimethoxy-2-nitroacetophenyldiazoethane was filtered directly into the NADP solution. The biphasic mixture was stirred vigorously for 10 h, and the chloroform layer was removed and replaced by fresh solution of the diazoethane derivative. The reaction was stirred overnight and monitored by HPLC to show complete consumption of NADP within 24 h. The organic phase was removed and the aqueous layer purified by HPLC **Method 2** using AG MP-1 resin developed with a gradient of water and TFA (0.1 M) (RT = 18 min, 45% TFA). The fractions were collected, neutralized to pH 7, and lyophilized to give a yellowish product (45 mg, 47%). $^{1}$H NMR ($D_2O$, 600 MHz): δ 9.34 (s, 1H), 9.18 (s, 1H), 8.86 (d, *J* = 7.8 Hz, 1H), 8.35 (d, *J* = 29.4 Hz, 1H), 8.26 (d, *J* = 14.4 Hz, 1H), 8.21 (t, *J* = 6 Hz, 1H), 7.44 (d, *J* = 27.6 Hz, 1H), 6.93 (d, *J* = 6.6 Hz, 1H), 6.09 (d, *J* = 5.4 Hz, 1H), 6.03 (d, *J* = 5.4 Hz, 1H), 5.87 (d, *J* = 6 Hz, 1H), 5.63(m, 1H), 5.1 (m, 1H), 4.53 (m, 1H), 4.48 (m, 1H), 4.4(m, 2H), 4.24 (m, 1H), 4.15–3.95 (m, 4H), 3.78 (m, 6H), 1.35 (d, *J* = 6 Hz, 3H). $^{31}$P NMR ($D_2O$, pH 7.4, 162 MHz): δ –.82, −10.49. Structure and NMR shown in Figure S5.

**Synthesis of caged NAADP analogs—**To a solution of DMNPE-caged NADP (19 mg, 0.02 mmol) in water (3 ml) was added a solution of one of these; nicotinic acid, 4-methyl nicotinic acid, 5-methyl nicotinic acid, 5-amino nicotinic acid, or 5-thiomethyl nicotinic acid ( 0.2 mmol) in water (3 ml). The mixture was adjusted to pH 4 and stirred at 37 °C in the presence of *Aplysia* ADP-ribosyl cyclase (150 μl, 0.2 g/ml) described in [50] and [51]. The reaction was monitored by HPLC and showed complete loss of DMNPE-caged NADP and formation of caged NAADP analog after 24 h. The product was purified by HPLC **Method 2** using anion exchange AG MP-1 and developing the chromatography with an aqueous TFA gradient (0.1 M). The fractions were collected, neutralized to pH 7, and lyophilized and stored at −80°C. The synthetic procedure and properties of each analog are reported in Table 2. The NMR data for each caged analog are given below. Structures, representative NMR spectra, HPLC traces, and HRMS are provided in Supplementary Material Figures S6–S10.

**Caged NAADP (1):** $^{1}$H NMR ($D_2O$, 600 MHz): δ 9.40 (s, 1H), 9.23 (s, 1H), 8.96 (d, *J* = 7.8 Hz, 1H), 8.36 (d, *J* = 24 Hz, 1H), 8.26 (d, *J* = 14.4 Hz, 1H), 8.21 (t, *J* = 6 Hz, 1H), 7.44 (d, *J* = 24 Hz, 1H), 6.93 (d, *J* = 7.8, 1H), 6.1 (d, *J* = 5.4 Hz, 1H), 6.03 (d, *J* = 5.4 Hz, 1H), 5.87 (d, *J* = 6 Hz, 1H), 5.64 (m, 1H), 5.1 (m, 1H), 4.54 (m, 1H), 4.47 (m, 1H), 4.4 (m, 2H), 4.25 (m, 1H), 4.16–4.0 (m, 4H), 3.79 (m, 6H), 1.35 (t, *J* = 3.6 Hz, 3H). $^{31}$P NMR ($D_2O$, pH 7.4, 162 MHz): δ –0.96, −10.77. HRMS calcd for $C_{31}H_{39}N_7O_{22}P_3^+$: 954.14, Found *m/z*: 954.11 (M+Na).

**Caged 4-Methyl NAADP (2):** $^{1}$H NMR ($D_2O$, 600 MHz): δ 8.98 (s, 1H), 8.85 (s, 1H), 8.65 (s, 1H), 8.33 (d, *J* = 23.4 Hz, 1H), 8.15 (d, *J* = 12 Hz, 1H), 7.44 (d, *J* = 46.2 Hz, 1H), 6.92

(d, *J* = 10.8, 1H), 5.96 (m, 2H), 5.82 (d, *J* = 6 Hz, 1H), 5.69 (m, 1H), 5.13 (m, 1H), 4.54 (m, 1H), 4.44(m, 1H), 4.37 (m, 2H), 4.23 (m, 1H), 4.15–4.02 (m, 4H), 3.82 (m, 6H), 2.49 (s, 3H), 1.37 (t, *J* = 5.4 Hz, 3H). $^{31}$P NMR ($D_2O$, pH 7.4, 162 MHz): δ –0.80, −10.04. HRMS calcd for $C_{32}H_{41}N_7O_{22}P_3^+$: 968.15, Found *m/z*: 968.12 (M+Na).

**Caged 5-Methyl NAADP (3):** $^{1}$H NMR ($D_2O$, 600 MHz): δ 8.96 (s, 1H), 8.66 (t, *J* = 9.6 Hz, 2H), 8.31 (s, 1H), 7.95 (d, *J* = 15.6 Hz, 1H), 7.38 (d, *J* = 42 Hz, 1H), 6.91 (d, *J* = 12, 1H), 5.93 (s, 1H), 5.81 (m, 2H), 5.72 (m, 1H), 5.1 (m, 1H), 4.62(m, 1H), 4.45 (m, 1H), 4.36 (m, 3H), 4.23–4.17 (m, 4H), 3.88 (m, 6H), 2.49 (s, 3H), 1.43 (t, *J* = 5.4 Hz, 3H). $^{31}$P NMR ($D_2O$, pH 7.4, 162 MHz): δ –0.85, −10.12. HRMS calcd for $C_{32}H_{41}N_7O_{22}P_3^+$: 968.15, Found *m/z*: 968.17 (M+Na).

**Caged 5-Amino NAADP (4):** $^{1}$H NMR ($D_2O$, 600 MHz): δ 8.54 (d, *J* = 8.4 Hz, 1H), 8.45 (s, 1H), 8.40 (s, 1H), 8.35 (s, 1H), 8.27 (d, *J* = 13.8 Hz, 1H), 7.95 (s, 1H), 7.47 (d, *J* = 27 Hz, 1H), 6.96 (d, *J* = 9.6 Hz, 1H), 6.03 (d, *J* = 5.4 Hz, 1H), 5.87 (m, 2H), 5.66 (m, 1H), 5.1 (m, 1H), 4.53 (m, 1H), 4.41 (m, 1H), 4.38(m, 2H), 4.25 (m, 1H), 4.16–4.02 (m, 4H), 3.84 (m, 6H), 1.37 (d, *J* = 6 Hz, 3H). $^{31}$P NMR ($D_2O$, pH 7.4, 162 MHz): δ –1.14, −10.88. HRMS calcd for $C_{31}H_{41}N_8O_{22}P_3^+$: 969.15, Found *m/z*: 969.23 (M+).

**Caged 5-Thiomethyl NAADP (5):** $^{1}$H NMR ($D_2O$, 600 MHz): δ 9.11 (s, 1H), 8.87(s, 1H), 8.75 (t, *J* = 2.4 Hz, 1H), 8.41 (d, *J* = 6 Hz, 1H), 8.32 (d, *J* = 11.4 Hz, 1H), 7.5 (d, *J* = 23.4 Hz, 1H), 7.0 (d, *J* = 11.4 Hz, 1H), 6.09 (m, 2H), 5.92 (d, *J* = 5.4 Hz, 1H), 5.7 (m, 1H), 5.1 (m, 1H), 4.58 (m, 1H), 4.52 (m, 1H), 4.45 (m, 2H), 4.25 (m, 1H), 4.13–4.05 (m, 4H), 3.85 (m, 6H), 2.65 (s, 3H), 1.41 (d, *J* = 6.6 Hz, 3H). $^{31}$P NMR ($D_2O$, pH 7.4, 162 MHz): δ –. 1.17, −10.03. HRMS calcd for $C_{32}H_{41}N_7O_{22}P_3S$+: 1000.12, Found *m/z*: 1000.14 (M+Na).

**Synthesis of BZ194—**BZ194 was synthesized according to the original procedures described in [26]. The melting point and spectroscopic properties of the compound we isolated were in close agreement with the properties reported.

### 4.4 Cell culture

Human adeno-carcinoma SKBR3 cell line was purchased from ATCC (HTB-30) and cultured in phenol red-free McCoy's 5a medium (Fisher) with 10% fetal calf serum (Atlanta Biologicals) and split twice weekly.

### 4.5 Microinjection

Forty-eight hours prior to injection and live cell imaging experiments, SKRB3 cells were plated on glass bottom dishes (Mattek P50G-1.5-30-F) in phenol red-free McCoy's 5a medium. A Narishige IM-9B microinjector controlled by a Narishige NAI-2N micromanipulator was used for microinjection of single SKBR3 cells. Caged NAADP and its derivatives were diluted to their final concentration in intracellular buffer (10 mM Hepes, 128 mM KCl, 20 mM NaCl, 1mM $MgCl_2$, and 0.1 mM EGTA, pH 7.2) along with 200 μM of the $Ca^{2+}$ sensitive dye Fluo-4 and loaded (2μl) into glass micropipette (World Precision Instruments). Cells were co-injected with a mixture of the indicated concentration of caged NAADP or its analog and the $Ca^{2+}$ sensitive dye. In co-injection experiments, BZ194 was

dissolved in DMSO and mixed with the stock solution containing caged NAADP. A volume of approximately 1 nl was injected into each cell.

### 4.6 Microscopy and analysis of $[Ca^{2+}]_i$

After a short rest to allow the cells to recover from microinjection, determination of $[Ca^{2+}]_i$ was performed using digital fluorescence imaging microscopy with a monochronometer-based system and high speed CCD camera (TILL-Photonics). Cells were alternately excited at 488± 15 nm and the fluorescence emission was collected through a 510 ± 25-nm band pass filter (Chroma). Photolytic release of NAADP or analog was achieved using a pulsed xenon arc lamp fed to a dual port epifluorescence condenser using a fiber-optic guide (Rapp Optoelectronic JML-G2). Eight to ten 80-J, 0.5-ms flashes of UV light (360 ± 7.5 nm) were reflected onto the plane of focus using a DM400 dichroic mirror and Super Fluor 40×, 1.3 NA oil immersion objective

### 4.7 Analysis of NAADP signaling and binding in sea urchin egg homogenates

This was performed according to the procedure of Aarhus et al. [36]. Briefly, testing of NAADP or analogs for $Ca^{2+}$ release on cell free receptor systems in the presence and absence of antagonist was performed on homogenates (1.25% v/v) prepared from sea urchin eggs (*Strongylocentrotus purpuratus)* diluted with intracellular medium containing 250 mM potassium gluconate buffer (pH 7.2), 0.5 mM ATP, 4 mM creatinine phosphate, creatinine (phospho)kinase and 3 μM fluorescent indicator, Fluo-3. The dilutions and all experiments were conducted at 17 °C. Fluorescence was measured using a fluorescence plate reader (excitation 490 nm and emission 535 nm). In some cases, solutions of caged analogs were irradiated with UV light prior to testing. The competitive binding assays were done in triplicate in 96 well filter plates containing the cell free sea urchin egg homogenate and constant concentration of radioligand [$^{32}$P]NAADP (0.2 nM). The competitor and [$^{32}$P]NAADP were incubated simultaneously with the sea urchin egg homogenate for 90 min at 4 °C. The homogenate was filtered and washed and the radioactivity retained on the filter was determined by liquid scintillation [28].

### 4.8 Uncaging efficiency

To determine whether there were differences in the efficiency of uncaging for the synthesized analogs, we measured their photolysis rate under identical, controlled conditions. Stock solutions of pure caged NAADP analogs (685 μM) were prepared in intracellular buffer. A photolysis reaction was run for each analog simultaneously by placing 50 μl of the stock solution on a porcelain spot-test plate under a handheld short wave UV lamp (254 nm) for 10 minutes. Each sample (50 μl) was then analyzed by HPLC under the same conditions as for prior analyses. The analogs were partially uncaged and NAADP or its derivative peak was observed after the photolysis reaction. The ratio of the photolysed uncaged portion to the intact caged portion was calculated as a percentage. For UV treatment in experiments with sea urchin egg homogenates, compounds were irradiated in a Rayonet photochemical reactor (Southern New England Ultraviolet Co.) for 2 minutes [36].

## Supplementary Material

Refer to Web version on PubMed Central for supplementary material.

## Acknowledgments

Thank you to Dr. Surya Nauli for the use of his microinjection apparatus. This work was supported by a University of Toledo Interdisciplinary Research Initiation Program Grant and by NIH Grant # GM100444-01.

## References

1. Berridge MJ, Bootman MD, Roderick HL. Calcium signalling: dynamics, homeostasis and remodelling. Nat Rev Mol Cell Biol. 2003; 4:517–529. [PubMed: 12838335]
2. Berridge MJ, Lipp P, Bootman MD. The versatility and universality of calcium signalling. Nat Rev Mol Cell Biol. 2000; 1:11–21. [PubMed: 11413485]
3. Clapham DE. Calcium Signaling. Cell. 2007; 131:1047–1058. [PubMed: 18083096]
4. Berridge MJ. Inositol trisphosphate and calcium signalling. Nature. 1993; 361:315–325. [PubMed: 8381210]
5. Lee HC. Mechanisms of calcium signaling by cyclic ADP-ribose and NAADP. Physiol Rev. 1997; 77:1133–1164. [PubMed: 9354813]
6. Guse AH. Regulation of Calcium Signaling by the Second Messenger Cyclic Adenosine Diphosphoribose (cADPR). Curr Mol Med. 2004; 4:239–248. [PubMed: 15101682]
7. Fliegert R. Regulation of calcium signalling by adenine-based second messengers. Biochem Soc Trans. 2007; 35:109–114. [PubMed: 17233614]
8. Lee HC. Cyclic ADP-ribose and Nicotinic Acid Adenine Dinucleotide Phosphate (NAADP) as Messengers for Calcium Mobilization. J Biol Chem. 2012; 287:31633–31640. [PubMed: 22822066]
9. Clapper DL, Walseth TF, Dargie PJ, Lee HC. Pyridine nucleotide metabolites stimulate calcium release from sea urchin egg microsomes desensitized to inositol trisphosphate. J Biol Chem. 1987; 262:9561–9568. [PubMed: 3496336]
10. Lee HC, Aarhus R. A Derivative of NADP Mobilizes Calcium Stores Insensitive to Inositol Trisphosphate and Cyclic ADP-ribose. J Biol Chem. 1995; 270:2152–2157. [PubMed: 7836444]
11. Cancela JM, Churchill GC, Galione A. Coordination of agonist-induced $Ca^{2+}$-signalling patterns by NAADP in pancreatic acinar cells. Nature. 1999; 398:74–76. [PubMed: 10078532]
12. Bak J, Billington RA, Timar G, Dutton AC, Genazzani AA. NAADP receptors are present and functional in the heart. Curr Biol. 2001; 11:987–990. [PubMed: 11448777]
13. Bak J, White P, Timár G, Missiaen L, Genazzani AA, Galione A. Nicotinic acid adenine dinucleotide phosphate triggers $Ca^{2+}$ release from brain microsomes. Curr Biol. 1999; 9:751–754. [PubMed: 10421579]
14. Cheng J, Ysufi ANK, Thompson MA, Chini EN, Grande JP. Nicotinic Acid Adenine Dinucleotide Phosphate: A New $Ca^{2+}$ Releasing Agent in Kidney. J Amer Soc Nephrology. 2001; 12:54–60.
15. Langhorst MF, Schwarzmann N, Guse AH. $Ca^{2+}$ release via ryanodine receptors and $Ca^{2+}$ entry: major mechanisms in NAADP-mediated $Ca^{2+}$ signaling in T-lymphocytes. Cell Signal. 2004; 16:1283–1289. [PubMed: 15337527]
16. Berg I, Potter BVL, Mayr GW, Guse AH. Nicotinic Acid Adenine Dinucleotide Phosphate ($NAADP^{+}$) Is an Essential Regulator of T-Lymphocyte $Ca^{2+}$-Signaling. J Cell Biol. 2000; 150:581–588. [PubMed: 10931869]
17. Lee HC. Nicotinic Acid Adenine Dinucleotide Phosphate (NAADP)-mediated Calcium Signaling. J Biol Chem. 2005; 280:33693–33696. [PubMed: 16076847]
18. Chini EN, Beers KW, Dousa TP. Nicotinate Adenine Dinucleotide Phosphate (NAADP) Triggers a Specific Calcium Release System in Sea Urchin Eggs. J Biol Chem. 1995; 270:3216–3223. [PubMed: 7852407]

19. Chini EN, Dousa TP. Nicotinate-adenine dinucleotide phosphate-induced $Ca^{2+}$-release does not behave as a $Ca^{2+}$-induced $Ca^{2+}$-release system. Biochem J. 1996; 316:709–711. [PubMed: 8670142]
20. Galione A, Churchill GC. Interactions between calcium release pathways: multiple messengers and multiple stores. Cell Calcium. 2002; 32:343–354. [PubMed: 12543094]
21. Lee HC, Aarhus R. Functional visualization of the separate but interacting calcium stores sensitive to NAADP and cyclic ADP-ribose. J Cell Sci. 2000; 113:4413–4420. [PubMed: 11082034]
22. Churchill GC, Okada Y, Thomas JM, Genazzani AA, Patel S, Galione A. NAADP Mobilizes $Ca^{2+}$ from Reserve Granules, Lysosome-Related Organelles, in Sea Urchin Eggs. Cell. 2002; 111:703–708. [PubMed: 12464181]
23. Berridge G, Dickinson G, Parrington J, Galione A, Patel S. Solubilization of Receptors for the Novel $Ca^{2+}$-mobilizing Messenger, Nicotinic Acid Adenine Dinucleotide Phosphate. J Biol Chem. 2002; 277:43717–43723. [PubMed: 12223470]
24. Macgregor A, Yamasaki M, Rakovic S, Sanders L, Parkesh R, Churchill GC, Galione A, Terrar DA. NAADP Controls Cross-talk between Distinct $Ca^{2+}$ Stores in the Heart. J Biol Chem. 2007; 282:15302–15311. [PubMed: 17387177]
25. Hohenegger M, Suko J, Gscheidlinger R, Drobny H, Zidar A. Nicotinic acid-adenine dinucleotide phosphate activates the skeletal muscle ryanodine receptor. Biochem J. 2002; 367:423–431. [PubMed: 12102654]
26. Dammermann W, Zhang B, Nebel M, Cordiglieri C, Odoardi F, Kirchberger T, Kawakami N, Dowden J, Schmid F, Dornmair K, Hohenegger M, Flügel A, Guse AH, Potter BVL. NAADP-mediated $Ca^{2+}$ signaling via type 1 ryanodine receptor in T cells revealed by a synthetic NAADP antagonist. Proc Natl Acad Sci USA. 2009; 106:10678–10683. [PubMed: 19541638]
27. Trabbic C, Walseth TF, Slama JT. Synthesis, Biochemical Activity, and Structure-Activity Relationship Among Nicotinic Acid Adenine Dinucleotide Phosphate (NAADP) Analogs. Messenger. 2012; 1:108–120.
28. Jain P, Slama JT, Perez-Haddock LA, Walseth TF. Nicotinic Acid Adenine Dinucleotide Phosphate Analogues Containing Substituted Nicotinic Acid: Effect of Modification on $Ca^{2+}$ Release. J Med Chem. 2010; 53:7599–7612. [PubMed: 20942470]
29. Lee HC, Aarhus R. Structural Determinants of Nicotinic Acid Adenine Dinucleotide Phosphate Important for Its Calcium-mobilizing Activity. J Biol Chem. 1997; 272:20378–20383. [PubMed: 9252343]
30. Billington RA, Tron GC, Reichenbach S, Sorba G, Genazzani AA. Role of the nicotinic acid group in NAADP receptor selectivity. Cell Calcium. 2005; 37:81–86. [PubMed: 15541466]
31. Morgan AJ, Galione A. Investigating cADPR and NAADP in intact and broken cell preparations. Methods. 2008; 46:194–203. [PubMed: 18852050]
32. Lin-Moshier Y, Walseth TF, Churamani D, Davidson SM, Slama JT, Hooper R, Brailoiu E, Patel S, Marchant JS. Photoaffinity Labeling of Nicotinic Acid Adenine Dinucleotide Phosphate (NAADP) Targets in Mammalian Cells. J Biol Chem. 2012; 287:2296–2307. [PubMed: 22117075]
33. Parkesh R, Vasudevan SR, Berry A, Galione A, Dowden J, Churchill GC. Chemo-enzymatic synthesis and biological evaluation of photolabile nicotinic acid adenine dinuclotide phosphate ($NAADP^{+}$). Org & Biomol Chem. 2007; 5:441–443. [PubMed: 17252124]
34. Lee HC, Aarhus R, Gee KR, Kestner T. Caged Nicotinic Acid Adenine Dinucleotide Phosphate: Synthesis and Use. J Biol Chem. 1997; 272:4172–4178. [PubMed: 9020130]
35. Aarhus R, Graeff RM, Dickey DM, Walseth TF, Hon CL. ADP-ribosyl Cyclase and CD38 Catalyze the Synthesis of a Calcium-mobilizing Metabolite from NADP. J Biol Chem. 1995; 270:30327–30333. [PubMed: 8530456]
36. Aarhus R, Dickey DM, Graeff RM, Gee KR, Walseth TF, Lee HC. Activation and Inactivation of Ca Release by NAADP. J Biol Chem. 1996; 271:8513–8516. [PubMed: 8621471]
37. Schrlau MG, Brailoiu E, Patel S, Gogotsi Y, Dun NJ, Bau HH. Carbon nanopipettes characterize calcium release pathways in breast cancer cells. Nanotechnology. 2008; 19:325102–325102. [PubMed: 21828806]

38. Brailoiu E, Churamani D, Cai X, Schrlau MG, Brailoiu GC, Gao X, Hooper R, Boulware MJ, Dun NJ, Marchant JS, Patel S. Essential requirement for two-pore channel 1 in NAADP-mediated calcium signaling. J Cell Biol. 2009; 186:201–209. [PubMed: 19620632]
39. Albrieux M, Lee HC, Villaz M. Calcium Signaling by Cyclic ADP-ribose, NAADP, and Inositol Trisphosphate Are Involved in Distinct Functions in Ascidian Oocytes. J Biol Chem. 1998; 273:14566–14574. [PubMed: 9603972]
40. Malgaroli A, Milani D, Meldolesi J, Pozzan T. Fura-2 Measurement of Cytosolic Free Ca $^{2+}$ in Monolayers and Suspensions of Various Types of Animal Cells. J Cell Biol. 1987; 105:2145–2155. [PubMed: 3680375]
41. Dammermann W, Guse AH. Functional Ryanodine Receptor Expression Is Required for NAADP-mediated Local Ca2+ Signaling in T-lymphocytes. J Biol Chem. 2005; 280:21394–21399. [PubMed: 15774471]
42. Naylor E, Arredouani A, Vasudevan SR, Lewis AM, Parkesh R, Mizote A, Rosen D, Thomas JM, Izumi M, Ganesan A, Galione A, Churchill GC. Identification of a chemical probe for NAADP by virtual screening. Nat Chem Biol. 2009; 5:220–226. [PubMed: 19234453]
43. Churchill GC, Galione A. NAADP induces $Ca^{2+}$ oscillations via a two-pool mechanism by priming IP3- and cADPR-sensitive $Ca^{2+}$ stores. EMBO J. 2001; 20:2666–2671. [PubMed: 11387201]
44. Cancela JM, Van Coppenolle F, Galione A, Tepikin AV, Petersen OH. Transformation of local Ca2+ spikes to global Ca2+ transients: the combinatorial roles of multiple Ca2+ releasing messengers. The EMBO journal. 2002; 21:909–919. [PubMed: 11867519]
45. Coumans FA, van Dalum G, Beck M, Terstappen LW. Filter characteristics influencing circulating tumor cell enrichment from whole blood. PloS one. 2013; 8:e61770. [PubMed: 23626725]
46. Walseth TF, Lin-Moshier Y, Jain P, Ruas M, Parrington J, Galione A, Marchant JS, Slama JT. Photoaffinity Labeling of High Affinity Nicotinic Acid Adenine Dinucleotide Phosphate (NAADP)-Binding Proteins in Sea Urchin Egg. J Biol Chem. 2012; 287:2308–2315. [PubMed: 22117077]
47. Walseth TF, Lin-Moshier Y, Weber K, Marchant JS, Slama JT, Guse AH. Nicotinic Acid Adenine Dinucleotide 2-Phosphate (NAADP) Binding Proteins in T-Lymphocytes. Messenger. 2012; 1:86–94.
48. Axelxon JT, Bodley JW, Walseth TF. A volatile liquid chromatography system for nucleotides. Anal Biochem. 1981; 116:357–360. [PubMed: 7316167]
49. Wilcox M, Viola RW, Johnson KW, Billington AP, Carpenter BK, McCray JA, Guzikowski AP, Hess GP. Synthesis of photolabile precursors of amino acid neurotransmitters. J Org Chem. 1990; 55:1585–1589.
50. Munshi C, Lee HC. High-level expression of recombinant Aplysia ADP-ribosyl cyclase in Pichia pastoris by fermentation. Protein Expr Purif. 1997; 11:104–110. [PubMed: 9325145]
51. Lee HC, Graeff RM, Munshi CB, Walseth TF, Aarhus R. Large-scale purification of Aplysia ADP-ribosylcyclase and measurement of its activity by fluorimetric assay. Methods Enzymol. 1997; 280:331–340. [PubMed: 9211328]

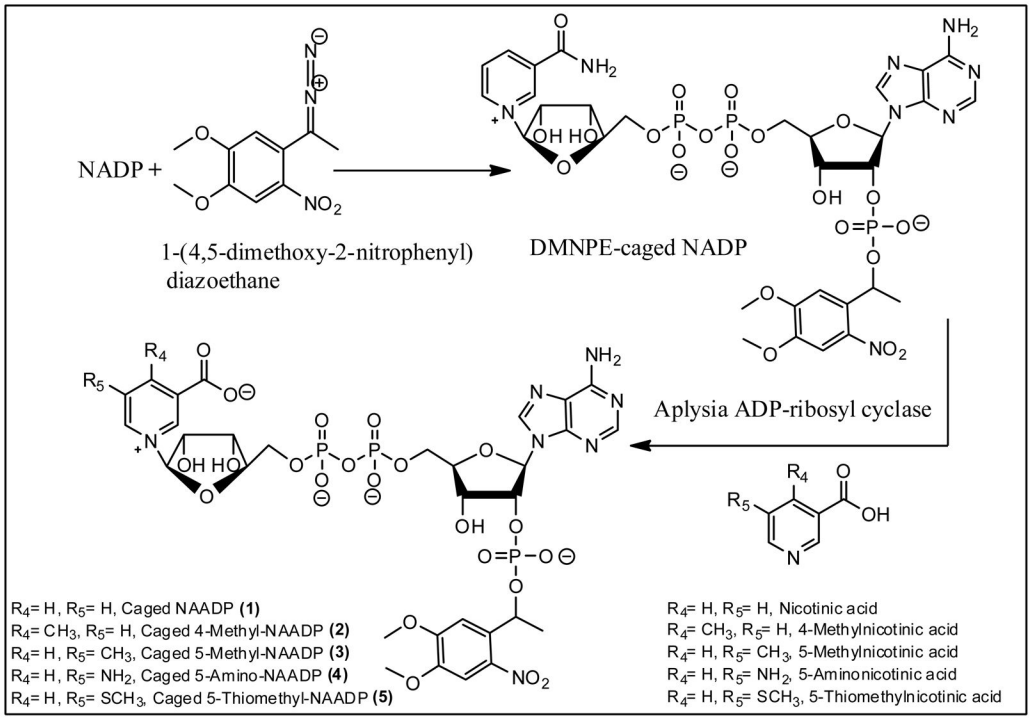


**Figure 1.**
Chemo-enzymatic synthesis of novel caged NAADP analogs.

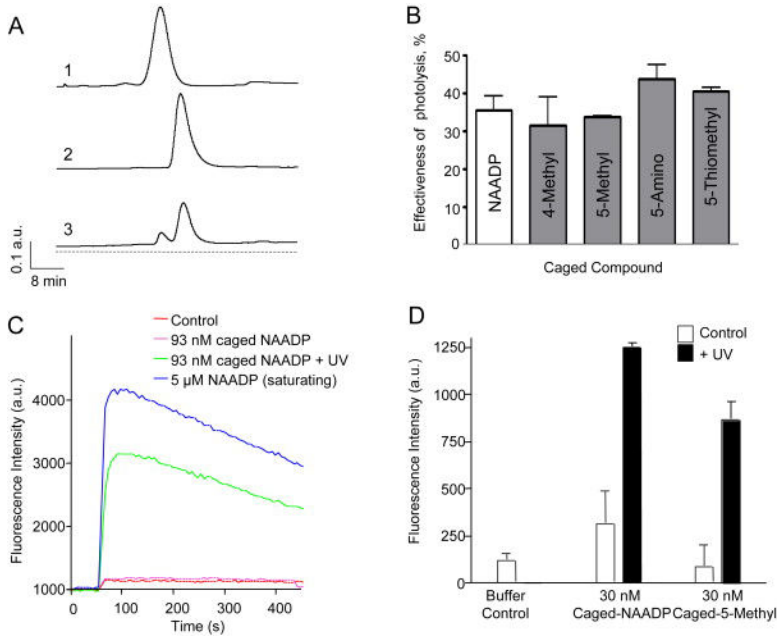


**Figure 2.**

UV photolysis of caged NAADP analogs (**1–5**). (A) HPLC traces of 50 µl samples of 685 µM (1) NAADP, (2) caged NAADP before photolysis reaction, and (3) caged NAADP after photolysis reaction resulting in the appearance of a liberated NAADP peak. (B) Photolysis efficiency of different caged NAADP analogs. Data shows the portion of uncaged compound of each analog expressed as percent of total compound after 10 min photolysis reaction; mean data of three experiments. (C) Fluorometric $Ca^{2+}$ release traces from Fluo-3 labeled sea urchin *Strongylocentrotus purpuratus* egg homogenates after addition of 5 µM NAADP, 93 nM caged NAADP, or 93 nM caged NAADP treated with UV light prior to addition (D) Peak fluorescence intensity following addition as in (C) of caged NAADP or caged 5-methyl-NAADP directly (Control) and with prior UV treatment (+UV).

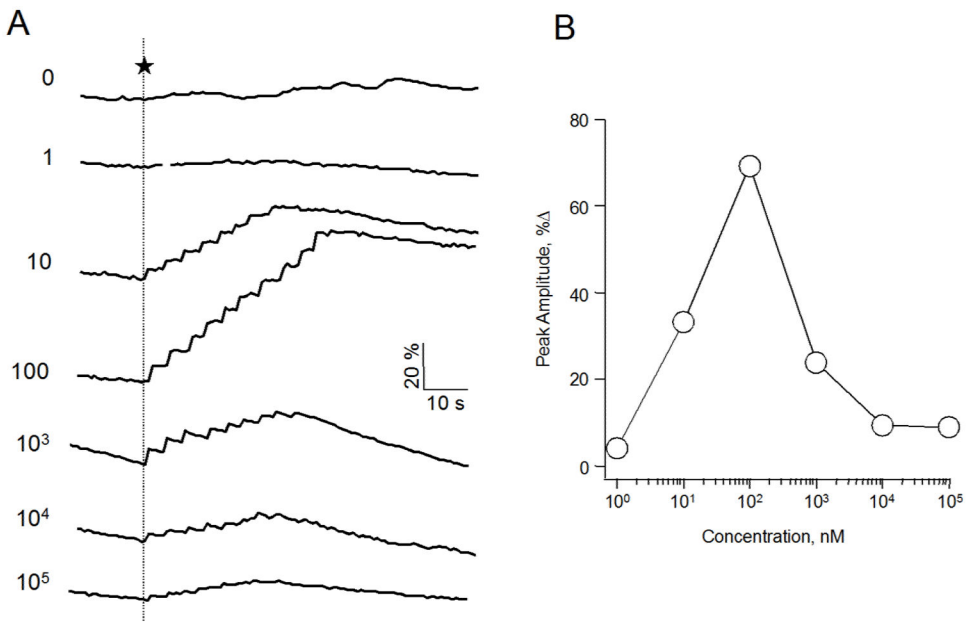


**Figure 3.**

NAADP-mediated $Ca^{2+}$ signaling in SKBR3 cells. (A) Representative fluorometric traces of $Ca^{2+}$ release in single SKBR3 cells induced by the photolysis of caged NAADP. Cells were co-injected with a mixture of the indicated concentration in nM of caged NAADP and the $Ca^{2+}$ sensitive dye Fluo-4 (200 μM). Free cytosolic $Ca^{2+}$ was measured after applying 8–10 flashes of UV light to release active NAADP (indicated by dotted line). (B) The % increase from baseline of the peak amplitude of each trace presented in A.

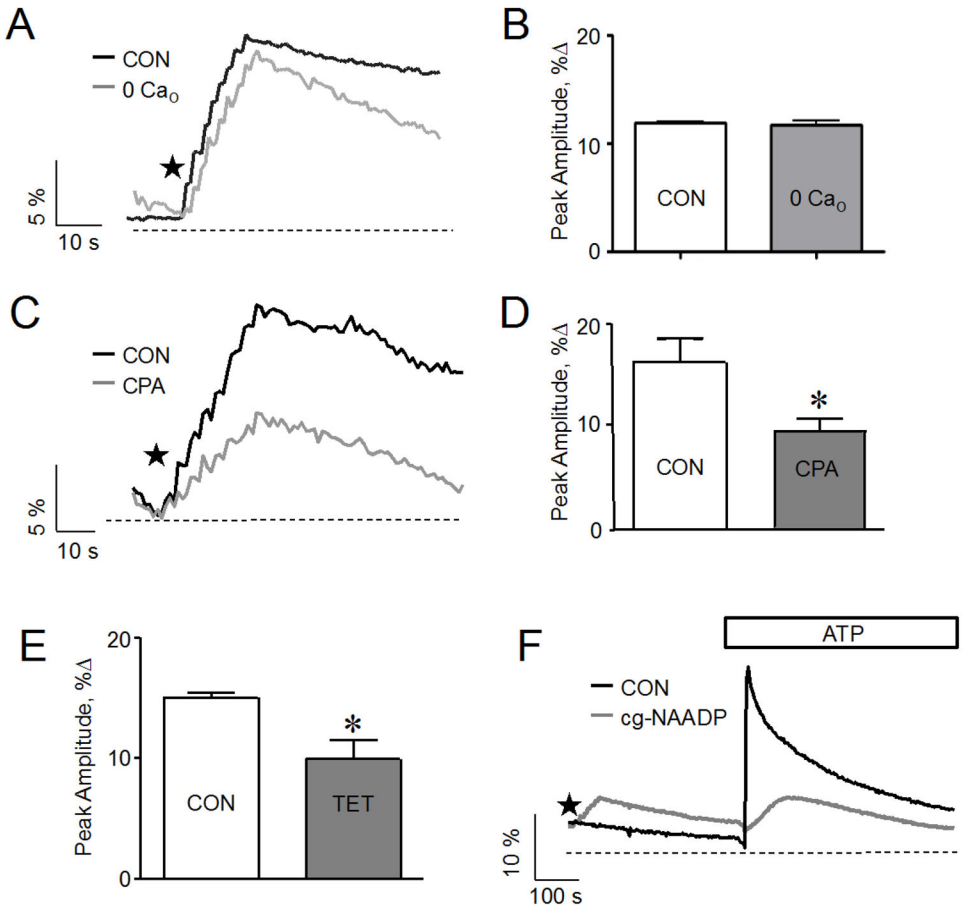


**Figure 4.**

Effect of a reduction in extracellular or ER $Ca^{2+}$ on $Ca^{2+}$ signals evoked by the photolysis of caged NAADP in SKBR3 cells. (A) $Ca^{2+}$ release response to the photolysis of caged NAADP (100 nM) in $Ca^{2+}$ free medium (0 $Ca_o$) and control medium (CON). (B) The cumulative data from (A) plotted as % increase of the $Ca^{2+}$ peak relative to baseline; mean data of 3–5 experiments; $p > .05$. (C) Reduction of $Ca^{2+}$ signals induced by the photolysis of caged NAADP (100 nM) following pretreatment with CPA (1 μM) for 30–40 minutes compared to control (CON). (D) The cumulative data from (C) plotted as % increase of the $Ca^{2+}$ peak relative to baseline; mean data of 3–5 experiments; *, $p < .05$. (E) Decrease in $Ca^{2+}$ signals induced by the photolysis of caged NAADP (100 nM) following pretreatment with tetracaine (100 μM) for 20 minutes compared to control (CON); data plotted as % increase of the $Ca^{2+}$ peak relative to baseline; mean data of 3–5 experiments; *, $p < .05$. (F) $Ca^{2+}$ response to ATP application without (black line) or following (gray line) photolysis of caged NAADP (100 nM). The amount of $Ca^{2+}$ released by extracellular ATP (100 μM) from the ER is lowered if the response to photoreleased NAADP occurred prior to ATP addition. Stars indicate application of sequential flash uncagings.

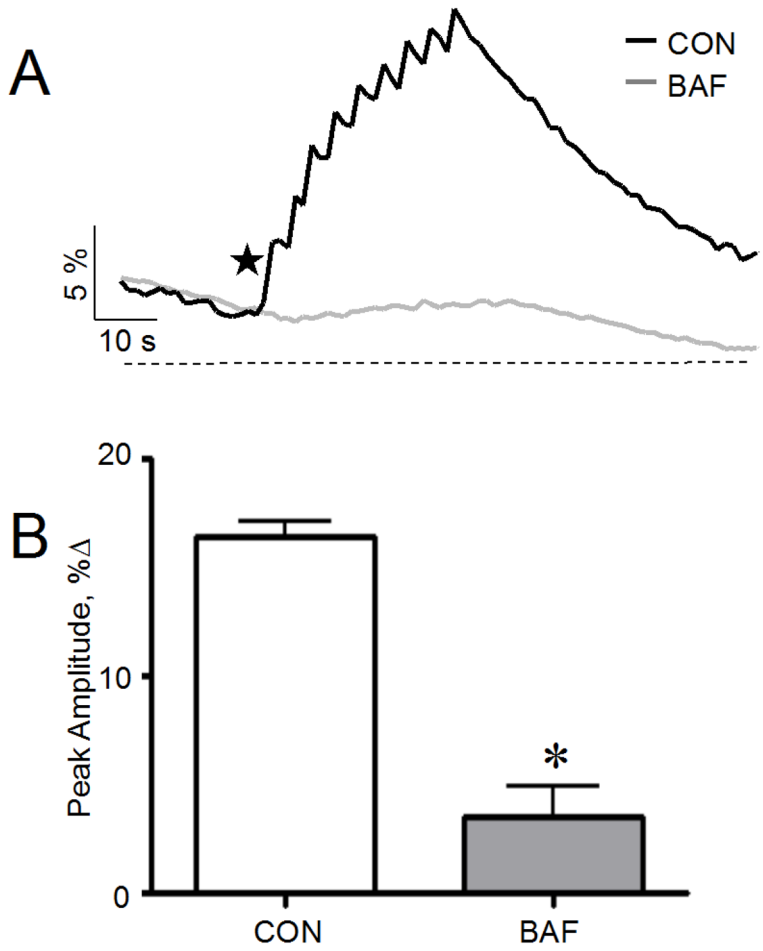


**Figure 5.**

Effect of bafilomycin A1 on $Ca^{2+}$ signals evoked by photolysis of caged NAADP in SKBR3 cells (A) Abolishment of $Ca^{2+}$ signals evoked by photolysis of caged NAADP (100 nM) following bafilomycin A1 (1 μM) treatment. (B) The cumulative data from (A) plotted as % increase of the $Ca^{2+}$ peak relative to baseline; mean data of 3–5 experiments; *, $p < .05$. Star indicates sequential flash uncagings.

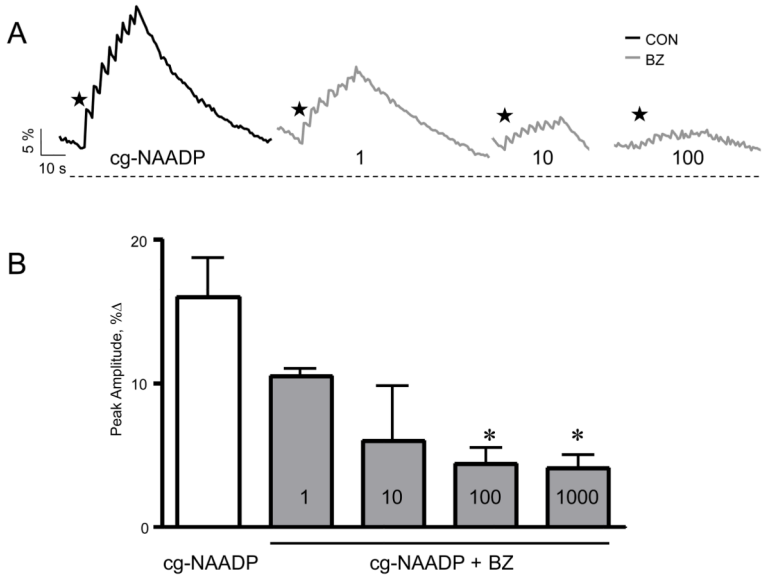


**Figure 6.**

Effect of BZ194 on NAADP-mediated $Ca^{2+}$ signaling in SKBR3 cells. (A) $Ca^{2+}$ signals evoked by photolysis of caged NAADP in SKBR3 cells co-injected with BZ194. SKBR3 cells were co-injected with a solution containing Fluo 4 (200 μM), caged NAADP (100 nM), and one of the indicated increasing concentrations in μM of BZ194. (B) Concentration-response curve of photolysed NAADP-induced $Ca^{2+}$ signaling following loading with the indicated concentration in μM of BZ194; mean data of 3–5 experiments; *, $p < .05$. Stars indicate application of sequential flash uncagings.

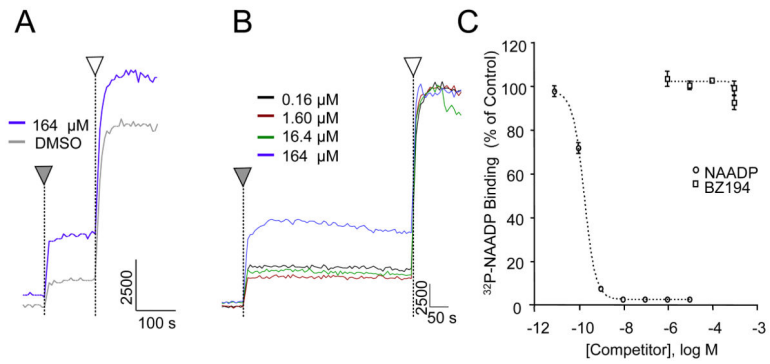


**Figure 7.**

Characterization of the antagonist activity of BZ194 on NAADP induced $Ca^{2+}$ release (A, B) and on competition ligand binding activity (C) in *Strongylocentrotus purpuratus* egg homogenates. (A, B) Fluorometric $Ca^{2+}$ release traces from sea urchin egg homogenates treated by the addition of DMSO alone or by varying concentrations of BZ194 dissolved in DMSO (▼), according to the procedure of Aarhus et al. [36]. This treatment was followed by the addition of a saturating concentration of NAADP (1 μM) (□). Panel A compares the results obtained with the vehicle DMSO alone with that obtained by adding 164 μM BZ194 as a solution in DMSO. Panel B shows the result of a concentration response study in which the BZ194 concentration was varied. The apparent $Ca^{2+}$ mobilization at high BZ194 concentration is likely due to small amounts of $Ca^{2+}$ contamination in the antagonist since in no case did we observe significant inhibition of the maximal NAADP-induced $Ca^{2+}$ release. (C) The competition radioligand binding curve for NAADP and BZ194 in sea urchin egg homogenates. The ability of NAADP (○) or BZ194 (▫) to compete with [$^{32}$P]NAADP for specific binding to sea urchin microsomes was determined according to the procedure of Aarhus et al. [36].

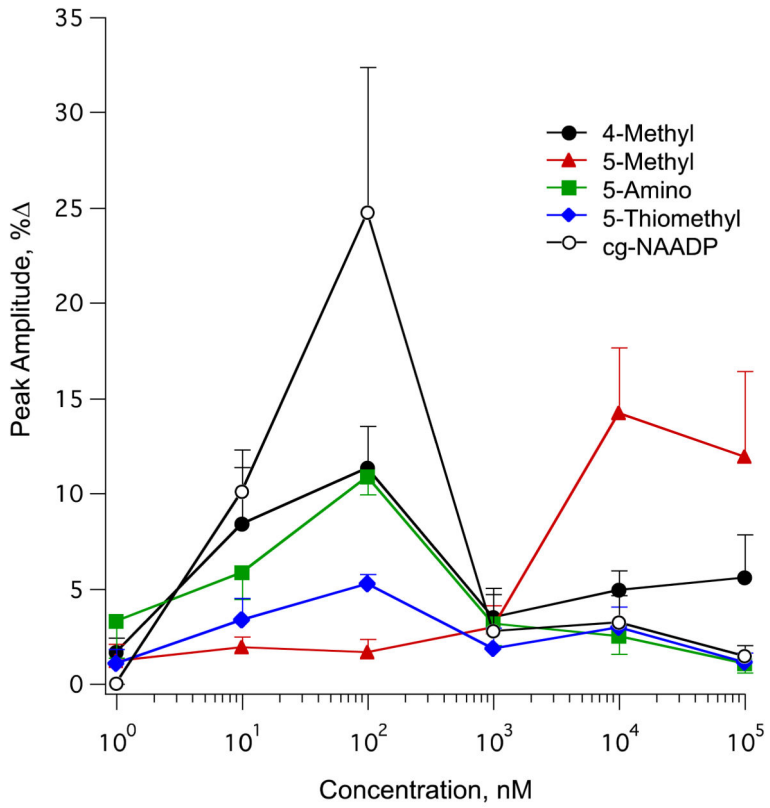


**Figure 8.**

Concentration–response curves for photolysed NAADP analogs (**1–5**) in SKBR3 cells. Curves depict the average peak of $Ca^{2+}$ concentration attained from SKBR3 cells following photolysis of (**1**) NAADP, (**2**) 4-methyl NAADP, (**3**) 5-methyl NAADP, (**4**) 5-amino NAADP, and (**5**) 5-thiomethyl NAADP. Each plotted point represents the mean of a minimum of three experiments.

## Table 1

Comparison of the potency and efficacy of pyridine substituted NAADP derivatives between sea urchin egg homogenate and SKBR3 cells.

| | Sea urchin[a] | | Human SKBR3 cells | |
|---|---|---|---|---|
| **Nicotinic acid substituent on NAADP** | **Fold increase in $EC_{50}$ compared to NAADP** | **Agonist efficacy** | **Fold increase in $[cmpd]_{optimum}$ vs. $[NAADP]_{optimum}$** | **Agonist efficacy** |
| 5-Amino | 1.5 | Full | 1 | Partial |
| 5-Methyl | 2.3 | Full | 100 | Partial |
| 5-Thiomethyl | 5.0[b] | Partial[b] | 1 | Weak-partial |
| 4-Methyl | 2,200. | Partial | 1 | Partial |

[a] Derived from Jain et al. [28].

[b] Unpublished observations

**Table 2**

Synthesis and properties of caged NAADP analogs.

| Initial Reactant | Base Exchanged | Source of Base | Caged Product | Retention Time of Product | Yield |
|---|---|---|---|---|---|
| Caged NADP | Nicotinic Acid; 24.6 mg | Sigma-Aldrich | Caged NAADP (**1**) | 24 min, 53.5% TFA | 10 mg, 52% |
| | 4-Methyl Nicotinic Acid; 27.4 mg | Maybridge | Caged 4-Methyl NAADP (**2**) | 24.5 min, 54% TFA | 9.5 mg, 49% |
| | 5-Methyl Nicotinic Acid; 27.4 mg | Acros | Caged 5-Methyl NAADP (**3**) | 23 min, 53% TFA | 11 mg, 57% |
| | 5-Amino Nicotinic Acid; 27.6 mg | Combi-Blocks Inc | Caged 5-Amino NAADP (**4**) | 23.5 min, 53% TFA | 10 mg, 52% |
| | 5-Thiomethyl Nicotinic Acid; 33.8 mg | Synthesized (see description) | Caged 5-Thiomethyl NAADP (**5**) | 24.7 min, 54% TFA | 10 mg, 50% |